Pergamon

Int. J. Heat Mass Transfer. Vol. 38, No. 10, pp. 1735–1749, 1995

0017–9310/95 $9.50+0.00

0017–9310(94)00338–6

Effects of free stream turbulence intensity on heat and mass transfers at the surface of a circular cylinder and an elliptical cylinder, axis ratio 4

A. KONDJOYAN and J. D. DAUDIN

Institut National de la Recherche Agronomique, S.R.V.-Theix, 63122 St-Genes-Champanelle, France

(*Received* 7 *June* 1994 *and in final form* 30 *October* 1994)

Abstract—Effect of free stream turbulence intensity ranging from 1.5 to 40% and of air velocity ranging from 0.5 to 5.0 m s^{-1} on transfer coefficients has been measured for a circular cylinder ($d = 0.1$ m) and an elliptical cylinder ($a = 0.2$ m, $R = 4$) in cross-flow. The effect of turbulence intensity appeared to be as important as the influence of velocity and seemed to be independent of the pressure gradient and of the degree of turbulence isotropy. One relation for each of the two cylinders has been established to describe all the experimental data. It appeared also that the transfers are much less affected by the axis ratio of the cylinder than by the air flow properties.

INTRODUCTION

Heat or mass transfers between air and products are involved in many food industry processes. To control these processes one must know the mean transfer coefficients which determine the mean flux exchanges and hence the treatment lengths and functioning of the apparatus. It is also important to know the local values of these coefficients around the treated bodies as the transfer intensity affects temperature changes and water concentrations and consequently the local rates of enzymatic and microbial reactions. The heterogeneity of microbial growth and of colour and flavour changes has a direct influence on food product quality.

In order to study these air–product exchanges in conditions close to those found in food industries, the coefficients should be known in the following situations: (1) low air velocity (0.1–5 m s^{-1}), (2) turbulent flow, (3) bodies of complex, irregular and various shapes.

Most of the experiments reported in the literature have been performed on flat plates and circular cylinders placed in cross-flows in which turbulence intensities were close to 0%. Morgan [1] reviewed about 100 works of this type on the circular cylinder. Some papers also describe the influence of the free stream turbulence intensity on transfers coefficients.

On a circular cylinder

The influence of the turbulence intensity on the heat transfer coefficient at the stagnation point has been studied in refs. [2–5]. These works demonstrate that the heat transfer coefficient increases with turbulence intensity and that this effect is more intense when the Reynolds number is higher. The relations proposed in these references are given in the Table 1. In these works it is also specified that these results can be extended to a region around the stagnation point, the area of which varies depending on the author. The variables used are always $Tu\,Re$ or $Tu\sqrt{Re}$, but the form of the relations and the results are very different. For a Reynolds number of 100 000 and a variation of the turbulence intensity from 0 to 6%, the intensification is 50% according to ref. [2], 55% according to ref. [4], 64% according to ref. [5] and 77% according to ref. [3].

The same studies have been performed taking into account the mean transfers over the whole circular cylinder surface. The effects are similar to those existing at the stagnation point. Table 2 gives the different relations proposed by the authors. The equations differ much more than in the case when only the stagnation point is concerned. The difference from one author to another is also greater. For a Reynolds number of 10 000, the transfer intensification due to a turbulence intensity of 6% is 8% according to ref. [7], 11% according to ref. [8], 21% according to ref. [5] and 37% according to Zapp, quoted by Morgan [1].

On a flat plate, with a zero pressure gradient

Kestin *et al.* [9] found that the free stream turbulence intensity had no influence on heat transfers when the boundary layer was laminar, but that the transfers increased when a pressure gradient was induced in the flow. These results are still open to debate [3]. When the boundary layer is turbulent, authors agree that the free stream turbulence intensity increases the transfers with or without a pressure gradient [9, 10].

NOMENCLATURE

- a length of major axis of elliptical cylinder [m]
- c_p specific heat of air [J kg^{-1} K^{-1}]
- D water diffusivity in air [m^2 s^{-1}]
- d cylinder diameter [m]
- d_{ref} diameter of the equivalent circular cylinder for an elliptical cylinder [m]
- E_1 methological errors on the determination of $\bar{h}$ and $\bar{k}$ by the psychrometric method
- h heat transfer coefficient [W m^2 K^{-1}]
- k mass transfer coefficient [kg m^{-2} (Pa s)$^{-1}$]
- k' mass transfer coefficient [m s^{-1}]
- K_{exp} experimental heat to mass transfer coefficient ratio
- K_{Theo} heat to mass transfer coefficient ratio coming from the relation of Lewis (Table 3)
- Le Lewis number
- L_{vap} latent heat of evaporation of water [J kg^{-1}]
- l_{ref} reference length [m]
- M_{air} 'molecular' weight of air [kg]
- M_{water} 'molecular' weight of water [kg]
- Nu Nusselt number $= hd/\lambda$
- P general symbol for pressure [Pa]
- P_{atm} atmospheric pressure [Pa]
- $P(T)$ saturated water vapour pressure at temperature T [Pa]
- Pr Prandtl number
- R major to minor axis ratio of an elliptical cylinder
- Re Reynolds number $= Ud/\nu$ or Ua/ν
- S body surface [m^2]
- Sh Sherwood number $= k'd/D$
- T air temperature [°C or K]
- T_{dew} dew point temperature [°C or K]
- Tu turbulence intensity of air in the main stream direction: $\sqrt{\overline{u^2}}/U_\infty$
- u velocity fluctuation around U [m s^{-1}]
- U velocity in the main stream direction outside the boundary layer [m s^{-1}]
- X curvilinear distance along the cylinder from the stagnation point or normal distance to the perforated plate [m].

Greek symbols

- ε plaster emissivity
- λ thermal conductivity of fluid [W m^{-1} K^{-1}]
- μ dynamic viscosity of fluid [kg m^{-1} s^{-1}]
- ν kinematic viscosity of fluid [m^2 s^{-1}]
- ρ_{air} density of air [kg m^{-3}]
- σ Stefan–Boltzmann constant [W m^{-2} K^{-4}]
- Φ_m mass flux exchanged between body surface and air [kg m^{-2} s^{-1}]
- Φ_{rad} heat flux exchanged by radiation [W m^{-2}]
- Φ_t heat flux exchanged by convection between body surface and air [W m^{-2}].

Subscripts

- A stagnation point of a cylinder
- w wall condition
- ∞ free stream condition
- 0 reference values of the dimensionless number for $Tu_\infty = 0\%$.

Mean

- $\bar{x}$ mean of x.

Table 1. Influence of the free stream turbulence intensity on the heat transfer coefficient at the stagnation point of a circular cylinder. Tu is in the decimal form. Nu_{A0} is the Nusselt number at the stagnation point for $Tu = 0\%$

Authors	Re, Tu	$(Nu_A - Nu_{A0})/Nu_{A0}$
Smith and Kuethe [2]	$0.1\% < Tu < 6.0\%$, $3\times10^4 < Re < 2.4\times10^5$	$0.0277(1-e^{-2.9\,10^{-5}Re})Tu\sqrt{Re}$ 'theory': $0.0277Tu\sqrt{Re}$
Dyban and Epick [3]	$500 < Tu\,Re < 7300$	$0.01\sqrt{Tu\,Re}$
Kestin and Wood [4]	$0.15\% < Tu < 7.20\%$ $75\times10^3 < Re < 125\times10^3$	$3.68\frac{Tu\sqrt{Re}}{100} - 4.21\left(\frac{Tu\sqrt{Re}}{100}\right)^2$
Dyban *et al.* [5]	$Tu\,Re < 9000$	$\frac{0.8Tu\,Re}{1500+Tu\,Re}$
Mujumdar, quoted by ref. [6]	$5000 < Re < 11\,000$ $0.5\% < Tu < 12\%$	$\frac{8\times10^{-4}Tu\,Re}{1.06}$

Table 2. Influence of the free stream turbulence intensity on the mean heat transfer coefficient of a circular cylinder. $Re_t = Tu\,Re$, Tu is in the decimal form

Authors	Tu (%)	Re	$(Nu-Nu_0)/Nu_0$	Reference point Nu_0
Zapp quoted by Morgan [1]	1–3	10 000	$1.29Tu^{0.500}$	?
	3–12	10 000	$2.42Tu^{0.667}$	?
Comings *et al.* [8]	1–7	1750–20 000	$\frac{Re^{0.07\left(1-\frac{1}{100Tu}\right)}}{1750}-1$	$Tu = 1\%$ $25.6\left(\frac{Re}{1750}\right)^{0.56}$
Endoh *et al.* [7]	4?–20?	10 000?–22 000?	$1.5\times10^{-6}Re_t\,Re^{0.5}\,Pr^{0.33}$	?
Dyban *et al.* [5]	0.3–12	2000–80 000	$Re^{(0.643Tu^{0.0125}-0.6)}-1$	$Tu = 0.3\%$ $0.262Re^{0.6}$

On an elliptical cylinder

To our knowledge the only study of the influence of turbulence on transfers has been performed by Seban [11]; the axis ratio of the cylinder was 4 and $56\,000 < Re < 236\,000$. His results indicate that the local heat transfers increase with the free stream turbulence intensity. However, Seban did not measure the turbulence intensity and gave only the characteristics of the grids he used to promote turbulence.

The conclusion to be drawn from the literature is that, if the increase of transfer coefficients with free stream turbulence intensity seems to be indisputable, the exact amount of increase remains unknown. Moreover, the turbulence intensity generated around the object is always less than 23% [5] and most of the time less than 12% [2, 4], Zapp quoted by ref. [1] and Mujumdar quoted by ref. [6]. However, measurements performed in a sausage dryer and a chilling room where the mean flow velocities were, respectively, 0.2 m s^{-1} and 0.4 m s^{-1} indicate that in the dryer the turbulence intensity was around 25%, with spatial variations between 17 and 29%, and in the chilling room the turbulence intensity was about 38% with spatial variations ranging from 22 to 60% [12].

The purpose of this work is to study the influence of free stream turbulence intensity from almost laminar to very turbulent flows on heat and mass transfer at the surface of a circular cylinder and an elliptical cylinder with a major to minor axis ratio of 4. The elliptical cylinder will enable to assess the influence of the body shape on the value of the transfer coefficients and hence the effect of the air flow properties for different pressure gradients induce by the body in the flow.

EXPERIMENTAL CONSIDERATIONS

Method

The method used to determine heat and mass transfer coefficients is based on psychrometry and is especially well adapted to bodies of complex shapes. Theoretical aspects and errors linked to data treatments and to measurements have been discussed in ref. [13]. The method consists in the drying of a fully wetted body in an air flow with constant properties. After a settling down period takes place a 'steady-state' or 'constant rate' period, which is clearly observable for capillary, porous non-hygroscopic materials [14, 15]. The fluxes exchanged between air and the wetted body surface are a convective and a radiative flux as well as an energy flux due to water evaporation. During the steady-state period the energy supplied to the surface exactly compensates the energy removed by evaporation. The air temperature, T_{air}, and the dew point temperature, T_{dew}, are measured during this period as are also the body surface temperatures, $\overline{T_w}$, and the body weight loss due to water evaporation, Φ_m. Little differences in temperature exist at the body surface. The maximum difference between any two points is 1.5°C and between two adjacent points 0.3°C. As in addition the conductivity of plaster is low, the heat flux exchanged by conduction and due to water migration from inside the body accounts for less than 2% of the total heat flux and hence can be neglected. The local transfer coefficients, h and k, are determined at the points where the temperature is measured, using the Lewis analogy [13, 16]. The mean heat and mass transfer coefficients, $\bar{h}$ and $\bar{k}$, are calculated using either the energy balance or by averaging the local values. The different stages of determination of the mean and local coefficients and the values of the methodological errors, E_{1h} and E_{1k} [17], are given in Table 3.

The samples used in these experiments were a circular cylinder 0.1 m in diameter and an elliptical cylinder of major axis length 0.2 m and axis ratio $R = 4$. The samples were made of plaster. In each sample, 13 thermocouples or Pt 100 probes were inserted 1 mm below the surface and located at regular intervals on half of the body perimeter. Before the experiment, the sample was soaked with the thermocouples or Pt 100 probes in place for at least 10 h in a water bath for hydration. Then the sample was inserted between plastic discs to prevent any transfer perpendicular to the main flow. Wooden discs were added to eliminate edge effects in the measurements areas (Fig. 1). The discs

Table 3. Stages of calculus of the mean and local transfer coefficients and of the methodological errors when using the psychrometric method

Successive stages of calculus	Relations used
Introduction of the measured variables	$\Phi_{m}, T_{w}, T_{\infty}, T_{dew}$
Determination of the mean transfer coefficients using: $\overline{T_w}$, $\overline{\phi_m}$	$\bar{h} = \frac{-\overline{\Phi_m} L_{vap}}{T_\infty - \overline{T_w}} - \varepsilon\sigma \frac{T_\infty^4 - \overline{T_w}^4}{T_\infty - \overline{T_w}}$ $\bar{k} = \frac{\overline{\Phi_m}}{P(T_{dew}) - P(\overline{T_w})}$
Theoretical ratio between heat and mass transfer coefficients	$K_{Theo} = \frac{C_p M_{air} P_{atm} Le^{2/3}}{L_{vap} M_{water}}$
Determination of the local transfer coefficients at each point where the temperature is measured	$h = \frac{\varepsilon\sigma(T_\infty^4 - T_w^4)}{T_w - T_\infty + \frac{P(T_w) - P(T_{dew})}{K_{Theo}}}$ $k = \frac{\varepsilon\sigma(T_\infty^4 - T_w^4)}{(K_{Theo}(T_w - T_\infty) + P(T_w) - P(T_{dew}))L_{vap}}$
Determination of the f values	$f = \frac{h}{\bar{h}} = \frac{k}{\bar{k}}$
Evaluation of the methodological errors on mean transfer coefficients	$E_{1h} = \int_s \left(\frac{f(T_w - \overline{T_w}) + \varepsilon\sigma \frac{T_w^4 - \overline{T_w}^4}{\bar{h}}}{s(T_\infty - \overline{T_w})} \right) ds$ $E_{1k} = \int_s \left(\frac{f(P(T_w) - P(\overline{T_w}))}{s(P(T_{dew}) - P(\overline{T_w}))} \right) ds$
Introducing the methodological errors when necessary	$\bar{h}_{cor} = \bar{h} + E_{1h}$ $\bar{k}_{cor} = \bar{k} + E_{1k}$
Determination of the experimental heat to mass transfer ratio	$K_{exp} = \frac{\bar{h}}{\bar{k} L_{vap}}$
Determination of the mean transfer coefficients by integration of the local values	$\overline{h_{int}} = \frac{1}{s} \int h \, ds$ $\overline{k_{int}} = \frac{1}{s} \int k \, ds$

were varnished and covered with a plastic film to prevent any evaporation from the wood surface. The cylinder was then placed cross-flow in the test cell of the wind tunnel. In the case of the elliptical cylinder, the major axis was parallel to the main flow direction.

During the experiments the air temperature and dew point temperature were kept steady around 35 and 5°C, respectively. The temperatures T_{air}, T_{dew} and T_w were measured every 2 min, and the body weight every 14 min. Careful attention was given to calibration: the temperatures were measured with an accuracy of ± 0.1°C and the body weight with an accuracy of ± 0.1 g.

Wind tunnel

The tunnel is a closed circuit wind tunnel specially designed and built for the psychrometric measurement of transfer coefficients in almost laminar to very turbulent flows (Fig. 2). The contraction area ratio between the settling chamber and the test section is nine. The test chamber measured 0.8×0.8 m with a length in the flow direction of 1.60 m. A three-axis traversing system enabled the automatic displacement of a probe in an area of chosen dimension and location with a preselected displacement step. The recording of the probe location and response was performed by a computer linked to the system.

The mean flow velocity and fluctuations were measured using a constant temperature hot wire anemometer. The hot wire element was 5 μm in diameter and 1.25 mm in length. The sample frequency was chosen between 0.5 and 2 kHz. Calibration of each wire probe with air temperature enabled mean velocity measurements to be made with an accuracy of 1–3% in the range of 0.5–5.0 m s^{-1} [17]. For high turbulence intensities the great amplitude of the velocity fluctuations could have generated non-linearity effects due to the thermal inertia of the hot wire [18].

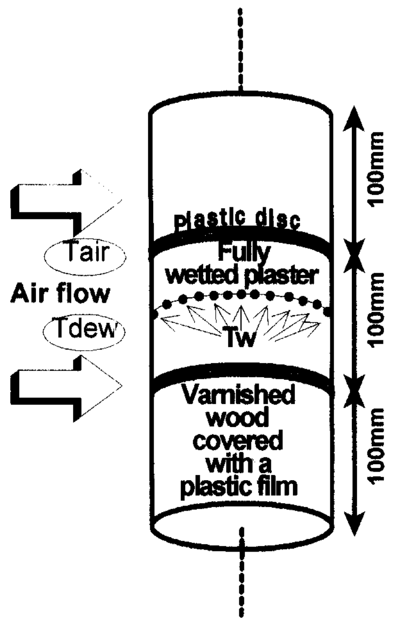

Fig. 1. Diagram of the samples.

But, as the frequencies of these fluctuations were low, this effect can be neglected. The component of the velocity fluctuation was measured in the main flow direction and in the transverse direction using, in addition to the previous 90°-wire probe, a single rotated 45°-wire probe [17, 18]. The turbulence isotropy in the flow was evaluated by the ratio $\overline{u^2}/\overline{v^2}$. As the method using the rotation of a 45°-wire probe is altered by the sensitivity of the wire to the fluctuation parallel to it, the turbulence was considered to be isotropic when $0.6 \leqslant \overline{u^2}/\overline{v^2} \leqslant 1.4$.

In a preliminary trial, air velocity and turbulence intensity were measured at 270 points in each of 25 cross-sections in the clear test chamber. The mean velocity at any point within the chamber differed by less than 0.5% from its average value over the entire chamber. It is always very difficult to have a low turbulence intensity and a homogeneous turbulence when the flow velocity is less than 2.0 m s^{-1}. In addition, usually when the flow turbulence intensity is low, the air and dew point temperatures are non-uniform across the chamber. In the most difficult conditions, with a main flow velocity of 0.5 m s^{-1}, only the area located at the middle top of the test chamber satisfied the initial objective of a homogeneous turbulence with an intensity less than 1.5%. This area was large enough to contain the sample and was called the experimental area. Its dimensions increased with air velocity to reach the totality of the test chamber for a value of 5.0 m s^{-1}. Attention was paid to the regulation of the air and dew point temperatures, so that these values were maintained uniform across the experimental area in the range of ± 0.1°C, even when the flow was laminar.

To promote turbulence, perforated plates were located normal to the flow in a drawer at the entrance of the test chamber. Perforated plates were chosen instead of grids because they enable one to generate a turbulence approximating a homogeneous and isotropic turbulence, even for a high level of turbulence intensity. The turbulence homogeneity was necessary in order to have the same flow conditions all around the sample. The turbulence isotropy is probably not a characteristic of the air flows which exist in industrial installations. However, it is easier from a fluid mechanics point of view to characterise the flow when the turbulence is isotropic. The nature of the turbulence downstream from a perforated plate cannot be determined theoretically but is known to depend on the perforation diameter Φ_g and on the perforated area, σ_g (expressed in percentage of the plate area). Plates with different values of Φ_g and σ_g were tested. During these experiments, the air flow velocity and turbulence intensity were measured at nine points in each of 20 cross-sections downstream from the plate. The

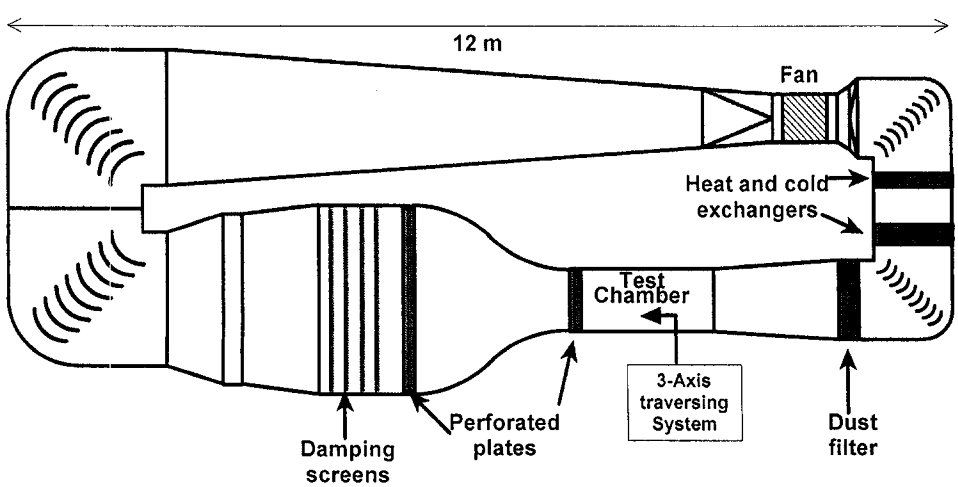

Fig. 2. Schematic representation of the wind tunnel.

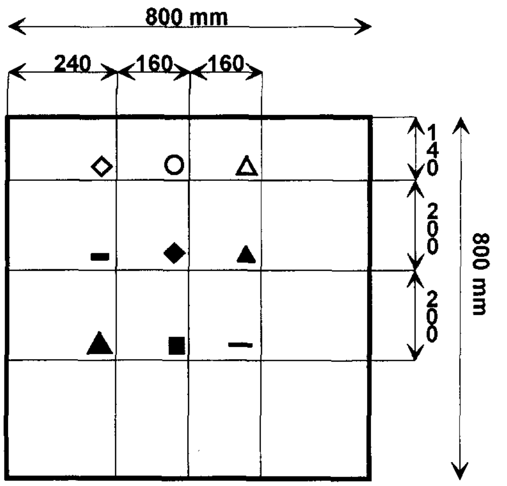

Fig. 3. Localization of the nine points of measurements in a section normal to the flow downstream from a perforated plate.

location of these points and their symbols are given in Fig. 3.

RESULTS AND DISCUSSION

Flow conditions

When the perforation diameter was less than 40 mm and the perforated area was 46% [plate no. 1, Fig. 4(a)], the turbulence was homogeneous downstream from the plates and the turbulence intensity decreased exponentially with the distance from the generator. This decrease is acknowledged as the behaviour characteristic of an isotropic turbulence downstream from grids [2, 4, 19, 20]. Measurements of the longitudinal and transverse fluctuations downstream from the perforated plates indicate that the turbulence seemed indeed to be very close to an isotropic turbulence. This plate was used to determine heat and mass transfer coefficients in flows with turbulence intensities close to 6%.

When the perforation diameter was 50 mm with a perforated area of 33% [plate no. 2, Fig. 4(b)], the exponential decrease of the turbulence intensity was restricted to the point located on the middle axis (X direction) of the test chamber. No decrease was observed on the border and at the top of the chamber, where the turbulence intensities were high and very different from one point to another. This plate was used to generate turbulence intensities ranging from 12 to 20%. In this case, the samples were centred on the middle axis of the test chamber, where the turbulence was close to that of a homogeneous and isotropic turbulence.

When the perforated diameter reached 100 mm with a perforated area of 6% [plate no. 3, Fig. 4(c)], the turbulence downstream from the plate was heterogeneous and not completely steady. It is difficult to characterize the turbulence in such a flow. The simplest way is to use the ratio $\sqrt{\overline{u^2}}/U_\infty$. This ratio was about 40% and is named in the following turbulence intensity even if in this case the word is improperly used from a fluid mechanics point of view. This flow which was not well defined from a fluid mechanics point of view was probably closer to the flows encountered in industrial installations.

For all the plates tested the turbulence intensity at any given point was nearly the same whatever the air velocity which ranged from 0.5 to 5.0 m s^{-1}.

The integral scale determined from the energy spectra varied from about 0.03 to 0.06 m when X increased from 0.2 to 1.5 m for plate no. 1 and from 0.06 to 0.16 m for plate no. 2.

The experimental schema is given in Table 4. Before each determination of the transfer coefficients, the air velocity was fixed. Then the region where the sample was to be located was scanned to measure the exact velocity and turbulence intensity values in that area. The mean values and the average deviation from these values are given in Table 5. The average deviation tended to be greater when the generated turbulence intensity was high, or for a given turbulence intensity for a low air velocity.

Effect of free stream turbulence intensity on mean transfer coefficients

When the psychrometric method is used, heat and mass transfer coefficients are determined simultaneously. Because of the Lewis relation their values written, respectively, in the form of Nusselt and Sherwood numbers should be the same apart from measurement errors. In this paper, except when specified otherwise, the results of heat and mass measurements are displayed with the same symbol.

No effect of the integral scale was evidenced. Hence in the following only the flow turbulence intensity is taken into account.

On the circular cylinder. The results of the 38 experiments are given in Fig. 5(a). From this figure two significant conclusions can be drawn:

(1) The intensification of transfers due to free stream turbulence exists for turbulence intensities up to 40%. For a given Reynolds number, the intensification of transfers is proportional to the turbulence intensity and does not seem to be affected by the turbulence isotropy or non-isotropy.

(2) The rate of intensification is greater for higher values of the Reynolds number. An increase of the turbulence intensity from 1.5 to 40% multiplies the

Table 4. Schema of the experiments

Cylinders	Turbulence intensity (%) 1.5	6.0	12	19	40
Circular	x	x	x	x	x
Elliptical (R = 4)	x		x		x

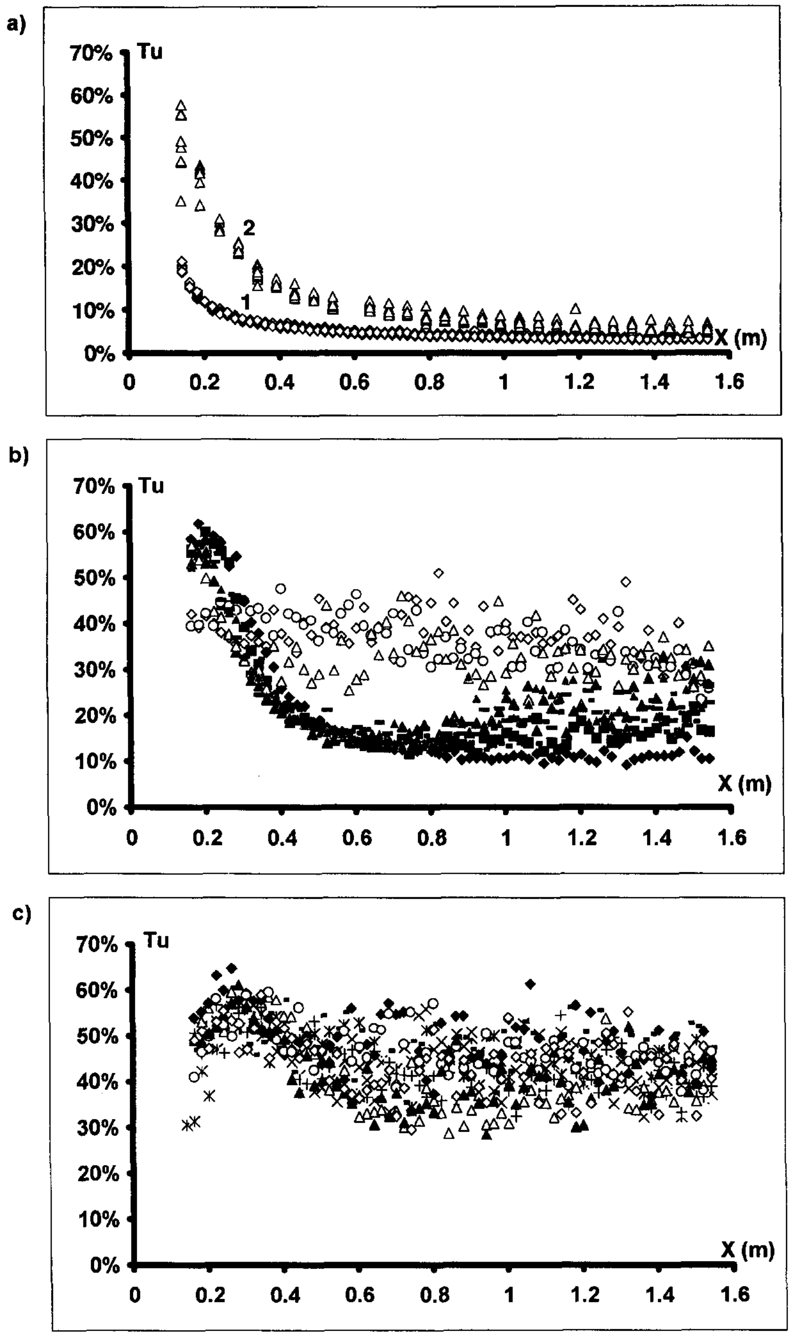

Fig. 4. Free stream turbulence intensity as a function of the distance X from the perforated plate. (a) (1) plate $\Phi_g = 18$ mm, $\sigma_g = 46\%$; (2) plate $\Phi_g = 40$ mm, $\sigma_g = 46\%$; for the sake of clarity the nine points of measurements are represented here by the same symbol. (b) $\Phi_g = 50$ mm, $\sigma_g = 33\%$. (c) $\Phi_g = 100$ mm, $\sigma_g = 6\%$. For (b) and (c) the symbols correspond to the measurements points defined in Fig. 3.

Nusselt number by 1.3 for a Reynolds number of 5000, and by 1.8 for a Reynolds number of 20 000.

Table 6 displays the values of A and n in the equations for heat and mass transfers: Nu (or Sh) $= A\,Re^n$, calculated for a given turbulence intensity. This type of correlation is very sensitive to the value of n. A variation of ± 0.005 of this value leads to a difference of 5–6% of the calculated Nusselt or Sherwood number. As the precision on the experimental results was generally better than that, the n values are given with three digits after the decimal point. For each turbulence intensity the 95% confidential limit was calculated [Fig. 5(a)]. The value of n increases regularly with turbulence intensity while the value of A decreases. The increase of n indicate that the higher

Table 5. Velocity (m s^{-1}) and turbulence intensity (mean value %, average deviation from the mean value) downstream from perforated plates in the area where the samples were located during the experiments

Plate features: Φ, σ Distance to the plate: X	Level of air velocity 1	2	3	4
$\Phi = 0.04$ m, $\sigma = 46\%$ $X = 1.50$ m	$V_\infty = 0.412 \pm 0.01$ $Tu_\infty = 5.1 \pm 0.1\%$	$V_\infty = 1.13 \pm 0.01$ $Tu_\infty = 5.8 \pm 0.1\%$	$V_\infty = 2.75 \pm 0.13$ $Tu_\infty = 6.4 \pm 0.1\%$	$V_\infty = 3.86 \pm 0.01$ $Tu_\infty = 6.3 \pm 0.1\%$
$\Phi = 0.04$ m, $\sigma = 46\%$ $X = 0.95$ m	$V_\infty = 0.419 \pm 0.01$ $Tu_\infty = 11.0 \pm 2\%$	$V_\infty = 1.20 \pm 0.02$ $Tu_\infty = 11.2 \pm 2.\%$	$V_\infty = 2.83 \pm 0.02$ $Tu_\infty = 11.4 \pm 2.0\%$	$V_\infty = 4.22 \pm 0.02$ $Tu_\infty = 11.4 \pm 2.0\%$
$\Phi = 0.05$ m, $\sigma = 33\%$ $X = 1.06$ m	$V_\infty = 0.51 \pm 0.01$ $Tu_\infty = 19.1 \pm 2\%$	$V_\infty = 1.52 \pm 0.02$ $Tu_\infty = 20.6 \pm 2.2\%$	$V_\infty = 3.54 \pm 0.08$ $Tu_\infty = 20.2 \pm 2.2\%$	$V_\infty = 5.28 \pm 0.5$ $Tu_\infty = 20.1 \pm 2.0\%$
$\Phi = 0.1$ m, $\sigma = 6\%$ $X = 1.55$ m	$V_\infty = 0.58 \pm 0.08$ $Tu_\infty = 35.1 \pm 4\%$	$V_\infty = 1.38 \pm 0.15$ $Tu_\infty = 41.6 \pm 4.6\%$	$V_\infty = 3.14 \pm 0.2$ $Tu_\infty = 43.1 \pm 4.0\%$	$V_\infty = 4.57 \pm 0.28$ $Tu_\infty = 42.8 \pm 3.3\%$

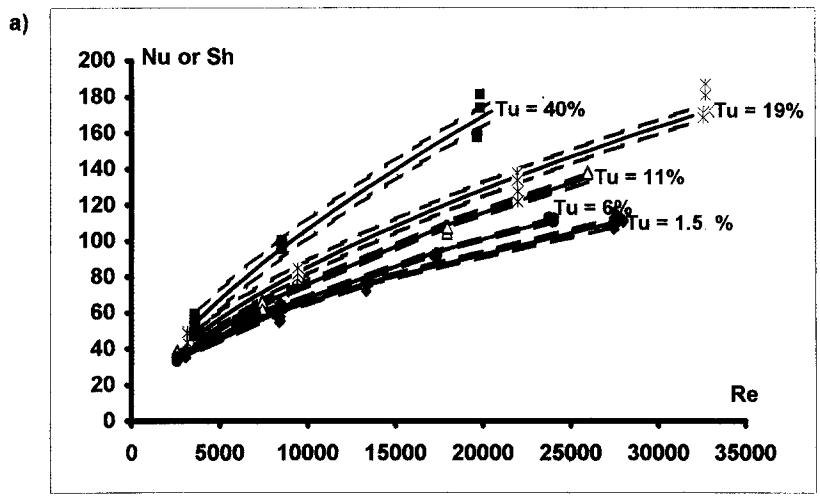

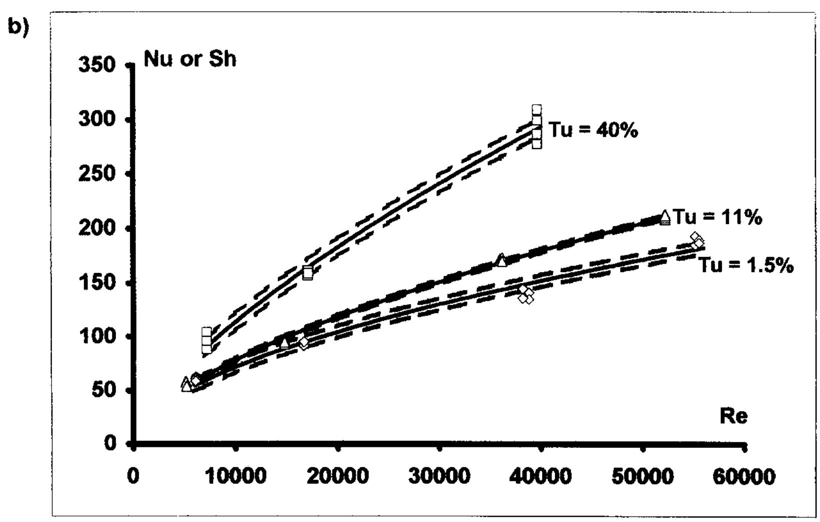

Fig. 5. Values of the transfer coefficients: (a) on the circular cylinder, for free stream turbulence intensities of 1.5, 6, 11, 19 and 40% ($I_{ref} = d$); (b) on the elliptical cylinder $R = 4$ ($I_{ref} = a$), for free stream turbulence intensities of 1.5, 11 and 40%. The dashed lines correspond to the calculated 95% confidential limit.

Table 6. A and n values in the relations $Nu = A\,Re^n$ ($4000 < Re < 30\,000$) for the circular cylinder in cross-flow with different turbulence intensities ($l_{ref} = d$)

Tu (%)	A	n
1.5	0.62	0.506
6.0	0.52	0.532
11.0	0.37	0.579
19.0	0.37	0.590
40.0	0.23	0.665

the Reynolds number the greater the transfer intensification. Linear regressions established for A and n as functions of turbulence intensity indicate that for a turbulence intensity of 0% the equation for heat and mass should be: Nu_0 (or Sh_0) $= 0.63Re^{0.50}$.

On the elliptical cylinder axis. The results of the 22 experiments are given in Fig. 5(b). The precision of the results is of the same order as in the case of the circular cylinder. The reference length chosen here is the length of the major axis ($l_{ref} = a$). As this dimension was twice the diameter of the circular cylinder, the Reynolds number appears to be greater but the observations are similar. An increase of the turbulence intensity from 1.5 to 40% multiplies the Nusselt number by 1.8 for a Reynolds number of 20 000 and by 1.94 for a Reynolds number of 40 000. The values of A and n in the equations Nu (or Sh) $= A\,Re^n$ are given in Table 7. Their variation is analogous to that of the circular cylinder. Moreover, the n values are very close whether the cylinder is circular or elliptical. Linear regressions established for A and n as functions of turbulence intensity indicate that for a turbulence intensity of 0% the equation for heat and mass should be: Nu_0 (or Sh_0) $= 0.67Re^{0.50}$.

Errors on the determination of mean transfer coefficients

For the circular cylinder the methodological errors, due to the variation of the transfer along the surface $E_{1h} = -0.8\%$ on $\bar{h}$ and $E_{1k} = +1.34\%$ on $\bar{k}$ (Table 3), were in conformity with the previous prediction [13] for an air temperature of 35°C and a hygrometry of 20%. Since these methodological errors were smaller than the experimental errors they were not taken into consideration. The experimental ratio of heat to mass transfer coefficient, K_{exp}, which is very sensitive to experimental errors, was 57.0 and thus very close to the value $K_{Theo} = 55.8$ calculated using the Lewis relation. These values were nearly the same ($K_{exp} = 56.0$, $K_{Theo} = 55.9$) when only the experiments for a Reynolds number greater than 17 000 were taken into account. When the free stream intensity was higher than 18% and the air velocity above 3.0 m s^{-1}, K_{exp} was greater than K_{Theo} by almost 5%. That could be explained by the very intensive drying which existed under these conditions at the surface of the cylinder. Then the water activity was probably no longer equal to one all around the body surface. This explanation is reinforced by the fact that it was very difficult to reach a long steady-state period at the stagnation point when the air velocity and turbulence intensity were respectively equal to 5.0 m s^{-1} and 40%. The determination of transfer coefficients was in this case a little less accurate.

On the elliptical cylinder the methodological errors, $E_{1h} = -2.3\%$ and $E_{1k} = +3.3\%$, were greater than on the circular cylinder. That seems to be reasonable because these errors depend on $\int_s f(T_w - \overline{T_w})$ and on $\int_s f(P(T_w) - P(\overline{T_w}))$ (Table 3) and thus on the distribution of the local coefficients at the body surface. On the circular cylinder this distribution is almost symmetric about the separation point, and the value of the local coefficient at the stagnation point is not too different from the other points. On the contrary, the local coefficient at the stagnation point of an elliptical cylinder is four to five times higher than on the other part of the surface, where the coefficients are almost constant. Hence the methodological errors were taken into account for the elliptical cylinder. After correction it appeared that K_{exp} was close to K_{Theo}. For the same reasons as in the case of the circular cylinder, the values of these ratios were identical when the Reynolds number was greater than 15 000 and were different by 5% when the exchanges were very intensive ($U_\infty = 5.0$ m s^{-1}, $Tu_\infty = 40\%$).

For both objects and low air velocities, heat could have been exchanged by free convection because of a difference in temperature between the body surface and the air of 10–20°C. The ratio Gr/Re^2, which is a criterion used to establish the dominant regions of free and forced convection [21], was less than 0.05 as soon as the air velocity was higher than 1.0 m s^{-1}. Thus, in our experiments the influence of free convection could be neglected except when the air velocity was 0.5 m s^{-1}. In this case, because of the experimental device, the possible air movement due to free convection should have been normal to the main flow direction. Hence it is very difficult to know if some exchange by free convection existed, and in this case if they have increased or decreased the exchange due to forced convection.

Table 7. A and n values in the relations $Nu = A\,Re^n$ ($5000 < Re < 55\,000$) for the elliptical cylinder in cross-flow with different turbulence intensities ($l_{ref} = a$)

Tu (%)	A	n
1.5	0.49	0.541
11.0	0.31	0.599
40.0	0.21	0.682

Comparison with literature

To compare with accuracy the values of the transfer coefficients in the literature, it is necessary to consider not only the experimental method used but also the exact flow conditions around the object. In particular, these conditions can be modified by the possible interactions between the body surface and the walls of the experimental chamber. Knudsen and Katz, quoted by ref. [1], assert that the only result of these interactions is an increase of the free stream velocity around the object, which can be taken into account by:

$$\frac{U_{\text{object}}}{U_{\text{chamber}}} = \sqrt{1 + \frac{d_{\text{object}}}{d_{\text{chamber}}}}. \tag{1}$$

d is the dimension of the object or of the test chamber and U represents the stream velocity with or without the object in the chamber. For a blockage ratio $d_{\text{object}}/d_{\text{chamber}}$ equal to 10, 20 and 40%, the increase of velocity is, respectively, 4.8, 9 and 18% according to equation (1). These increases do not seem to be so big and could be corrected by a simple measurement of the stream velocity. But according to West and Apelt [22] the phenomenon is much more complex as soon as the blockage ratio is greater than 6%, especially because of interactions between the wake of the cylinder and the chamber walls. This phenomenon is likely to influence the air–solid exchanges. Experimental studies on a circular cylinder (quoted by ref. [22]) have demonstrated, however, that the drag coefficient, which is very dependent on the flow conditions, is not affected as long as the blockage ratio is less than 16%.

Because of the small values of the aspect ratios of our samples (ratios of the length to the diameter of the cylinders) the results could have been altered, especially in the wake of the circular cylinder. This phenomenon is not a major restriction for the comparison with published results because most authors have used cylinders which aspect ratios are less than 5. However one must keep in mind that the present results obtained in the wake of the circular cylinder are perhaps slightly different from those on a near infinite circular cylinder.

Circular cylinder

The results of this study and results in the literature obtained with free stream turbulence intensities close to 0% and to 12% are given in Figs. 6 and 7, respectively. For a turbulence intensity near 0% (Fig. 6), the present results ($Tu = 1.5\%$) are a little in excess of those of Hilpert (quoted by ref. [1]) and of Whitaker (quoted by ref. [21]). This seems reasonable because the turbulence intensity was probably about 1% higher in our experiments than for Hilpert and Whitaker. However, the present results are lower than the results of Dyban *et al.* [5], which were obtained for a turbulence intensity of 0.3%. Moreover, the shape of the curve $Nu = A\,Re^n$, used by Dyban to describe his results, is very different from those of the other authors, whereas the shape of the curve of the present study is very close to that of Whitaker. The difference from Dyban's results was probably due to the large blockage ratio of 25% which existed in his wind tunnel. For a turbulence intensity close to 12% (Fig. 7), the difference between Dyban's results and the results of the present study (blockage ratio 12.3%) was the same as for a turbulence intensity of 0%. This similarity reinforces the previous explanation of a blockage effect on Dyban's results. In addition, results obtained in a pilot plant [23] where the turbulence intensity was 12% and the blockage ratio ranged from 17 to 40% are in between the present results and those of Dyban. Moreover, the slope of the curve obtained in the pilot plant is much more pronounced than that of Dyban.

Elliptical cylinder

The present results for a turbulence intensity of 12% and those obtained in the pilot plant [23] are given for the elliptical cylinder in Fig. 8. The results are presented using the Sherwood number to avoid the possible errors due to the evaluation of radiation. Because the blockage ratio for the elliptical cylinder in the pilot plant was only of 5–10% those results are very close to the present ones. The small differences can be explained by difficulties in the velocity regulation encountered in the pilot plant for low air velocities and by the lack of consideration of the methodological errors during the treatment of the data coming from the pilot plant.

Influence of the elliptical cylinder ratio on the mean transfer coefficient

To compare the exchanges at the surface of a circular and an elliptical cylinder one must choose a suitable reference length for the elliptical cylinder. The usual reference length found in literature is the length of the major axis. However, Ota *et al.* [24] suggest that one choose as reference length the diameter of the circular cylinder ('the equivalent' cylinder) d_{ref}, whose perimeter is the same as that of the elliptical cylinder. Thus the distance covered by the flow is the same along the surface of the two objects. The ratio between the diameter of the equivalent circular cylinder d_{ref} and the major axis of the elliptical cylinder a is [24]:

$$\frac{d_{\text{ref}}}{a} = \frac{2E'(r)}{\pi} \tag{2}$$

where $E'(r)$ is an associated complete elliptic integral of the second kind and $r^2 = 1 - R^{-2}$. The d_{ref}/a values calculated for the elliptical cylinder with ratios which range from 2 to 5 are given in Table 8. The substitution of a by d_{ref} in $Nu = A\,Re^n$ leads to the same relation with A' in place of A, where

$$A' = A\left(\frac{d_{\text{ref}}}{a}\right)^{1-n}.$$

When this substitution is performed in the equations of the Table 7, it appears that the mean Nusselt number at the surface of the elliptical cylinder ($R = 4$) is about 14% less than that of the equivalent circular cylinder. This result seems to be coherent with the

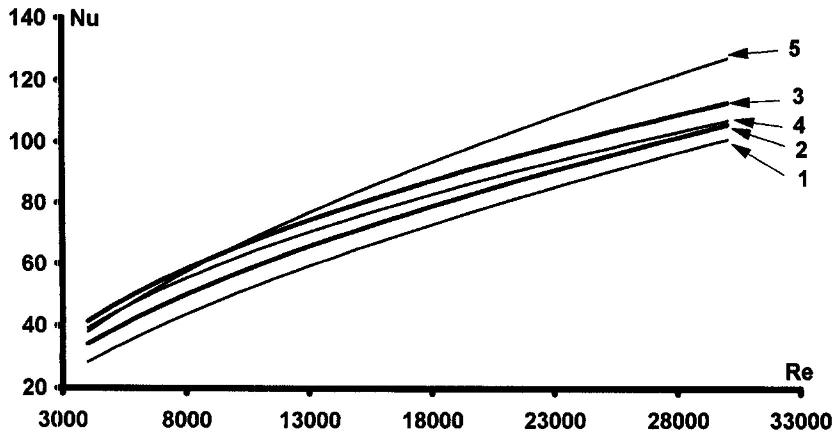

Fig. 6. Mean heat transfer coefficient on a circular cylinder in cross-flows of free stream turbulence intensities close to 0% (1) from Hilpert (quoted by ref. [1]); (2) from Whitaker (quoted by ref. [21]); (3) present results for $Tu = 1.5\%$; (4) extrapolated results for $Tu = 0\%$; (5) from Dyban *et al.* [5].

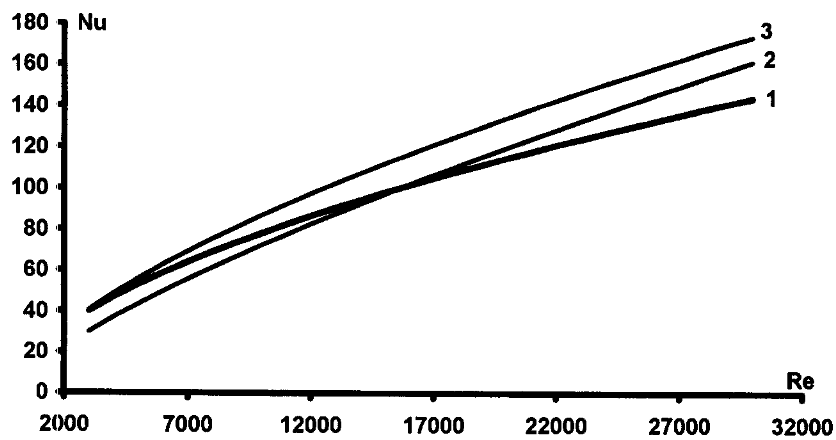

Fig. 7. Mean heat transfer coefficient on a circular cylinder in cross-flows of free stream turbulence intensities of 11–12%; (1) present results (blockage ratio 12%); (2) results in the pilot plant [23] (blockage ratio 17–40%); (3) from Dyban *et al.* [5] (blockage ratio 25%).

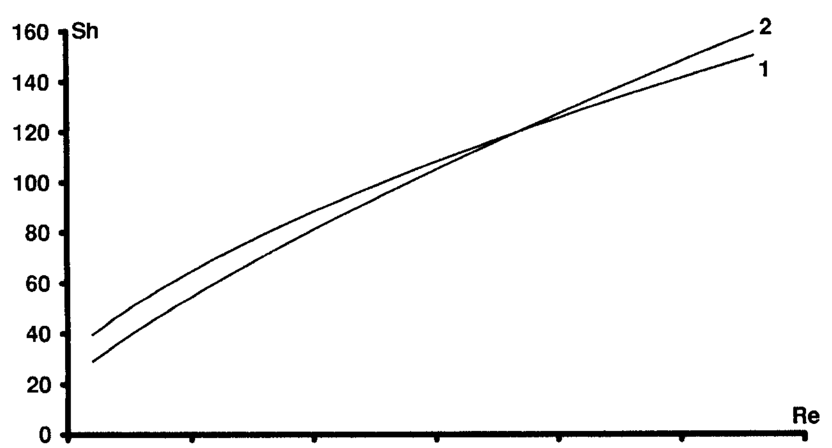

Fig. 8. Mean heat transfer coefficient on an elliptical cylinder ($R = 4$) in cross-flows of free stream turbulence intensities of 11–12%; (1) present results (blockage ratio less than 5%); (2) results in the pilot plant [23] (blockage ratio 5–10%).

Table 8. Ratio between the diameter of the equivalent cylinder d_{ref} and the length of the major axis of the elliptical cylinder a, for different values of R

R (major axis/minor axis)	d_{ref}/a
2	0.77
3	0.71
4	0.68
5	0.67

common knowledge on the development of boundary layers at the surface of circular and elliptical cylinders.

In any case, the effect of a four-fold multiplication of the elliptical cylinder ratio is much less than that produced by the variation of the free stream turbulence intensity from 11 to 40%, which can increase the Nusselt number by 60% for a Reynolds number of 40 000.

How are the transfers affected by the free stream turbulence intensity?

The results found in the literature raise some questions about the effect of free stream turbulence intensity on transfers: is this effect uniform at the surface of the cylinder? Is it influenced by the flow pressure gradient? Is this effect dependent on the nature of the boundary layer which develops at the body surface? The f function $f = h/\bar{h}$ is a useful guide to answer to these questions. The evolution of the local coefficients at the surface of the circular and the elliptical cylinders are given in Fig. 9(a) and (b), respectively, in the form

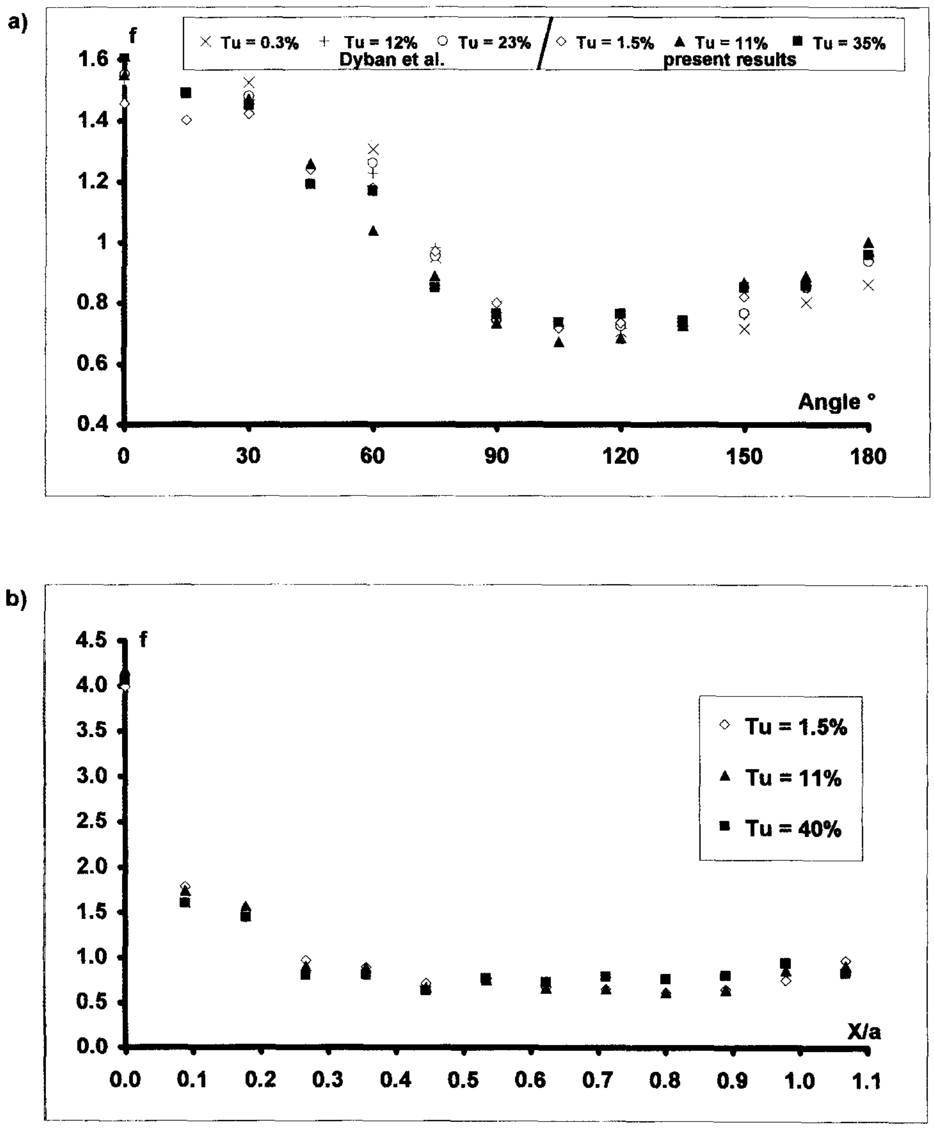

Fig. 9. Evolution of the local transfer coefficients in the form of f ($f = h/\bar{h}$) along the surface (main stream direction): (a) of the circular cylinder, comparison with Dyban's results for $Re = 4500$; (b) of the elliptical cylinder ($R = 4$); for: $0.5\ \mathrm{m\ s^{-1}} < U_{\infty} < 1.0\ \mathrm{m\ s^{-1}}$, $1.5\% < Tu_{\infty} < 40\%$.

of the f function for different turbulence intensities. The experimental errors on the f values were of the order of 5% when the air velocity was lower than $1.0\ \mathrm{m\ s^{-1}}$, which corresponded to a Reynolds number of 10 000. For a higher air velocity the psychrometric method became unusable for the determination of the local transfer coefficients because of an increase in the measurement errors [13]. The distribution of the local transfer coefficients on the circular cylinder is similar to the distribution obtained by Dyban *et al.* [5] for a Reynolds number of 4500. On the elliptical cylinder ($R = 4$) no comparison was possible with published results because of the lack of data for flows with different turbulence intensities.

Fig. 9(a) and (b) indicates that for $Re < 10\,000$ the values of the f function were the same for the free stream turbulence intensities ranging from 1.5 to 40%. Hence the effect of the turbulence intensity on transfers appears to have been the same at all points on the surface of the cylinders. That means also that the effect of turbulence did not depend on the pressure gradient and thus that this effect should have been the same on the circular and the elliptical cylinders. To test this idea, the ratios of intensification of the mean transfer coefficients on the two objects, Nu/Nu_0 and Sh/Sh_0, were described as functions of the two variables commonly used in the literature: $Tu\,Re$ and $Tu\sqrt{Re}$ [Fig. 10(a) and 10(b)]. The reference length chosen for the elliptical cylinder was, for this test, the diameter of the equivalent cylinder. Apart from the measurement errors, the intensification was similar whether the cylinder was circular or elliptical, and the experimental data were indisputably better described using $Tu\sqrt{Re}$. It is then possible to describe the transfer intensification on the two objects by a unique linear regression:

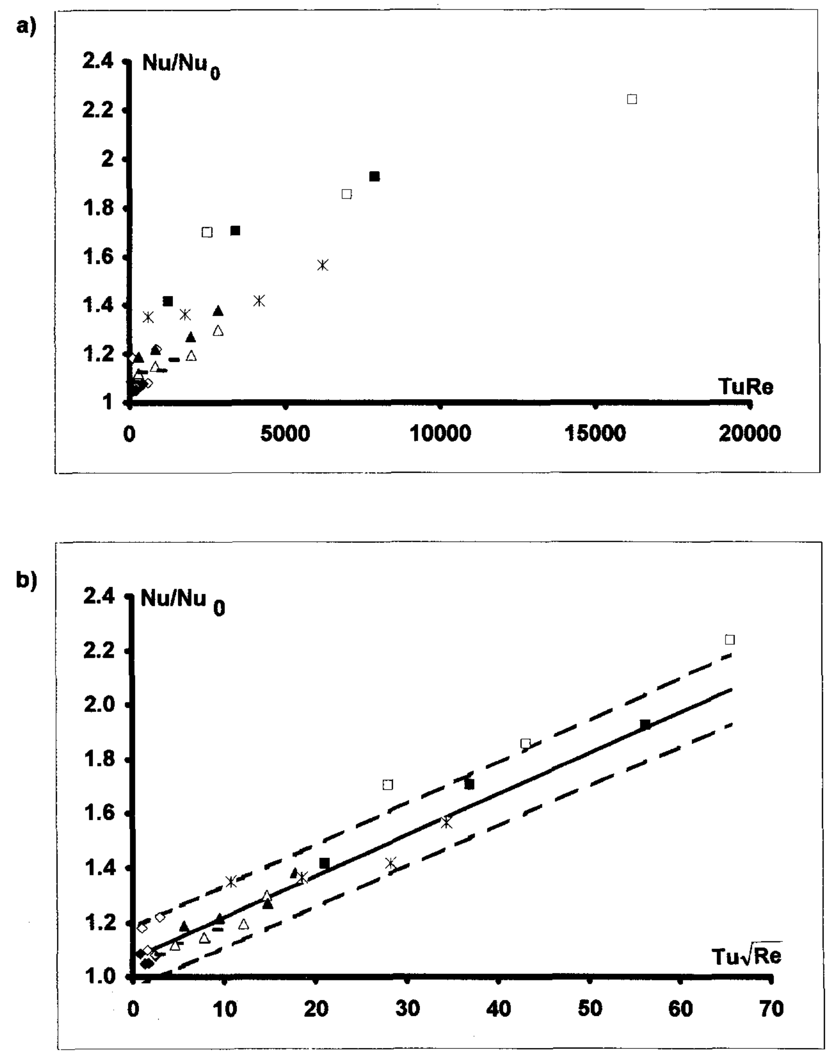

Fig. 10. Transfer intensification: Nu/Nu_0 for the circular and the elliptical cylinders: (a) described using $Tu\,Re$; (b) described using $Tu\sqrt{Re}$. The symbols are the same as in Fig. 11. The dash lines correspond to the calculated 95% confidential limit.

$$\frac{Nu}{Nu_0} \text{ or } \frac{Sh}{Sh_0} = 1.07+0.015Tu\sqrt{Re} \quad (3000 < Re < 33\,000). \quad (3)$$

One should keep in mind that for $Tu\sqrt{Re} > 40$ the results were obtained with a turbulence which was non-fully steady non-homogeneous and probably non-isotropic. In this case Tu represents only an assessment of the fluctuation in the mean flow direction.

Using equation (3) all the experimental results obtained on the circular and on the elliptical cylinders can be represented by two regressions, for $3000 < Re < 40\,000$ and $1\% < Tu < 45\%$:

$$Nu\,(\text{or } Sh) = (1.07+0.015Tu\sqrt{Re})0.63Re^{0.50} \quad \text{(circular)} \quad (4)$$

$$Nu\,(\text{or } Sh) = (1.07+0.015Tu\sqrt{Re})0.55Re^{0.50} \quad (\text{elliptical}, l_{\text{ref}} = d_{\text{ref}}). \quad (5)$$

The experimental values and the values calculated using equations (4) and (5) are given in Fig. 11. The average absolute difference between the experimental and the calculated values for the two cylinders is approximately 5%.

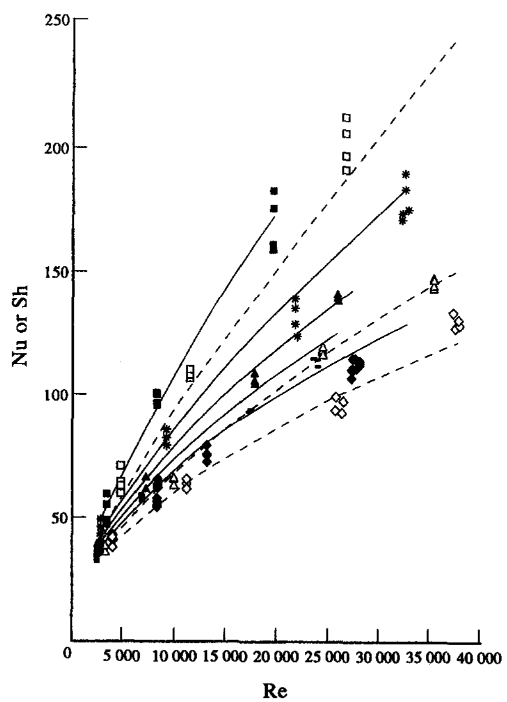

Fig. 11. Experimental mean transfer coefficients on the circular cylinder (solid symbols) and on the elliptical cylinder (open symbols). The calculated values coming from equation (4) are in solid lines and from equation (5) in dashed lines. (1) $Tu_\infty = 1.5\%$ (diamond); (2) $Tu_\infty = 6\%$ (dash); (3) $Tu_\infty = 11\%$ (triangle); (4) $Tu_\infty = 19\%$ (star); (5) $Tu_\infty = 40\%$ (square).

CONCLUSION

This study indicates that the transfers on both a circular and an elliptical cylinder are equally affected by the air velocity and by the turbulence intensity. The effect of the free stream turbulence intensity was important even for large turbulence intensities of the order of 40%.

The effect of free stream turbulence intensity seems to have been independent of the pressure gradient and of the degree of turbulence isotropy. Thus the intensification of transfers was described by a single relation for the circular and for the elliptical cylinders. Finally, two relations proportional to each other were used to describe all the experimental results in the range of $3000 < Re < 40\,000$, $1\% < Tu < 45\%$.

The influence of the elliptical cylinder ratio on the mean transfer coefficients values was much less than the effect of the air flow properties. If this conclusion is confirmed for bodies other than cylinders, the shape effect could be taken into account by a single factor provided that a suitable reference length can be found. Then the relations proposed in this paper corrected by a shape factor (experimentally determined at any turbulence intensity) could be used to calculate the exchanges at the surface of complex bodies.

This paper confirms that the local transfer coefficient is much higher at the stagnation point of an elliptical cylinder than elsewhere at the surface. It will be of great interest to know if similar discrepancies exist on bodies other than cylinders. Further studies would also be necessary to quantify the combined effect of free stream turbulence and blockage ratio on transfer coefficients. This subject is very important for transfers in packed beds and in exchanger design.

REFERENCES

1. V. T. Morgan, The overall convective heat transfer from smooth circular cylinders, *Adv. Heat Transfer* **11**, 199–264 (1975).
2. M. C. Smith and A. M. Kuethe, Effects of turbulence on laminar skin friction and heat transfer, *Phys. Fluids* **9**(12), 2337–2344 (1966).
3. E. P. Dyban and E. Ya. Epick, Some heat transfer features in the air flows of intensified turbulence. *Proc. 4th Heat Transfer Conf.* F.C.5.7, Part 2, Paris-Versailles (1970).
4. J. Kestin and R. T. Wood, The influence of turbulence on mass transfer from cylinders, *J. Heat Transfer* **93**, 321–327 (1971).
5. E. P. Dyban, E. Ya. Epick and L. G. Kozlova, Combined influence of turbulence intensity and longitudinal scale and air flow acceleration on heat transfer of circular cylinder, *5th Heat Transfer Conf.* F.C.8.4, pp. 310–314, Tokyo (1974).
6. M. I. Boulos and D. C. T. Pei, Heat and mass transfer from cylinders to turbulent fluid stream, *Can. J. Chem. Engng* **51**(12), 673–679 (1973).
7. K. Endoh, H. Tsuruga, H. Hirano and M. Morihira, Effect of turbulence on heat and mass transfer, *Jpn Res.* **1**, 113–115 (1972).
8. E. W. Comings, J. T. Clapp and J. F. Taylor, Air turbulence and transfer processes flow normal to cylinders, *Indust. Engng Chem.* **40**, 1076–1082 (1948).
9. J. Kestin, P. F. Maeder and H. E. Wang, Influence of

turbulence on the transfer of heat from plates with and without a pressure gradient. *Int. J. Heat Mass Transfer* **3,** 133–154 (1961).

10. S. Sugawara, T. Sato, H. Komatsu and H. Osaka, Effect of free stream turbulence on flat plate heat transfer. *Int. J. Heat Mass Transfer* **31,** 5–12 (1988).
11. R. A. Seban, The influence of free stream turbulence on the local heat transfer from cylinders. *J. Heat Transfer* **82,** 101–107 (1960).
12. J. D. Daudin and A. Kondjoyan, Influence de l'indice de turbulence de l'écoulement sur les procédés de traitement thermique de solides par l'air. *Réc. Prog. Génie Proc.* **5**(13), 287 (1991).
13. A. Kondjoyan and J. D. Daudin, Determination of transfer coefficients by psychrometry. *Int. J. Heat Mass Transfer* **36,** 1807–1818 (1993).
14. C. J. Geankoplis. *Transport Processes and Unit Operation.* Allyn and Bacon, Boston, MA (1983).
15. M. Loncin and R. L. Merson, *Food Engineering and Selected Applications*, p. 494. Academic Press, New York (1979).
16. W. K. Lewis, The evaporation of a liquid into a gas. *Trans. ASME* **15**(7), 445–446 (1922).
17. A. Kondjoyan, Contribution à la connaissance des coefficients de transferts de chaleur et de matière à l'interface air–solide. Thèse de Docteur de L'E.N.S.I.A. (1993).
18. G. Comte-Bellot, Anémométrie à fil chaud. Techniques de mesures dans les écoulements. *Eyrolles, Collection de la Direction des Etudes et Recherches d'Electricité de France*, pp. 117–198 (1974).
19. J. O. Hinze, *Turbulence.* McGraw-Hill, New York (1951), reissued (1987).
20. G. Comte-Bellot and S. Corrsin, The use of contraction to improve the isotropy of grid-generated turbulence. *J. Fluid. Mech.* **25,** 657–682.
21. N. M. Ozisik, *Heat Transfer, a Basic Approach.* McGraw-Hill, New York (1985).
22. G. S. West and C. J. Apelt, Blockage and aspect ratio effects on flow past a circular cylinder for $10^4 < Re < 10^5$. Research report N° CE29, Department of Civil Engineering University of Queensland (1981).
23. A. Kondjoyan, J. D. Daudin and J. J. Bimbenet, Heat and mass transfer coefficients at the surface of elliptical cylinders placed in a turbulent air flow. *J. Fd Engng* **20,** 339–367 (1993).
24. T. Ota, S. Aiba, T. Tsuruta and M. Kaga, Forced convection heat transfer from an elliptic cylinder of axis ratio 1 : 2, *Bull JSME* **26,** 262–267 (1983).